Journal of Power Sources 227 (2013) 86–93

Contents lists available at SciVerse ScienceDirect

Journal of Power Sources

journal homepage: www.elsevier.com/locate/jpowsour

Scaled-up synthesis of nanostructured Mg-based compounds and their hydrogen storage properties

Tong Liu [a], Hailong Shen [a], Yang Liu [b], Lei Xie [b], Jianglan Qu [b], Huaiyu Shao [b], Xingguo Li [b,*]

[a] Key Laboratory of Aerospace Materials and Performance (Ministry of Education), School of Materials Science and Engineering, Beihang University, Beijing 100191, China
[b] Beijing National Laboratory for Molecular Sciences (BNLMS), The State Key Laboratory of Rare Earth Materials Chemistry and Applications, College of Chemistry and Molecular Engineering, Peking University, Beijing 100871, China

HIGHLIGHTS

- We prepared the nanostructured Mg-based compounds by gas–solid reaction.
- The nanostructure of these compounds greatly enhances the sorption kinetics.
- The Mg_2Ni nanoparticles can absorb 0.95 H M^{-1} hydrogen in several minutes at 493 K
- The sorption kinetics of the nanostructured Mg_2Ni is stable during ten cycles.
- The thermodynamic properties of these nanostructured Mg_2M are improved slightly.

GRAPHICAL ABSTRACT

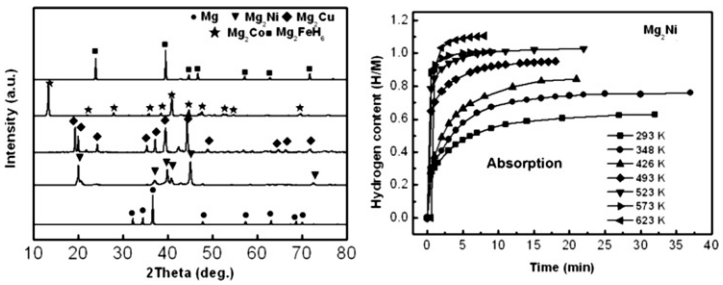

ARTICLE INFO

Article history:
Received 12 July 2012
Received in revised form
2 November 2012
Accepted 3 November 2012
Available online 16 November 2012

Keywords:
Mg-based compounds
Nanostructure
Hydrogen storage
Kinetics

ABSTRACT

Different from conventional method, we have produced nanoparticles of Mg, Fe, Co, Ni, Cu and other metals by hydrogen plasma metal reaction (HPMR) in semi-industrial scale. Using these elemental nanoparticles as raw materials, nanostructured Mg-based compounds with high purity including Mg_2Ni, Mg_2Co, Mg_2Cu and Mg_2FeH_6 are further synthesized by gas–solid reaction in much mild conditions. The Mg_2Ni nanoparticles of 50 nm can be prepared at 523 K under 4 MPa H_2. The formation mechanisms of the elemental nanoparticles during HPMR and the nanostructured Mg-based compounds during gas–solid reaction are discussed. The nanostructure of these samples greatly enhances the kinetic properties of hydrogen absorption and desorption. The Mg_2Ni nanoparticles can absorb hydrogen and saturate at 0.95 H M^{-1} (the number of hydrogen atoms per metal atom) in several minutes at 493 K. The sorption kinetics of the nanostructured Mg_2Ni is almost stable during ten cycles. The thermodynamic properties of these nanostructured Mg_2M are improved slightly.

1. Introduction

Although some new kinds of hydrogen storage materials such as amides, alanates, and borohydrides are intensively studied [1–3], Mg-based compounds are still thought to be promising for the practical applications in hydrogen storage [4–6] and battery electrode [7,8]. This is due to the great abundance and light weight of Mg, and the high hydrogen capacity of the hydrides e.g. 7.6 wt.% for MgH_2, 3.6 wt.% for Mg_2NiH_4, 4.5 wt.% for Mg_2CoH_5 and 5.4 wt.% for Mg_2FeH_6 [9]. However, one problem is their sluggish hydrogen sorption kinetics and relatively high thermodynamic stability, which results in the high absorption/desorption temperature of

* Corresponding author. Tel.: +86 10 6275 3691; fax: +86 10 6276 5930.
E-mail address: xgli@pku.edu.cn (X. Li).

0378-7753/$ – see front matter © 2012 Elsevier B.V. All rights reserved.
http://dx.doi.org/10.1016/j.jpowsour.2012.11.011

about 573 K, much higher than the operation temperature of fuel cell. The other problem is that it is hard to prepare Mg-based alloys, especially Mg_2Ni, Mg_2Co, Mg_2Cu and Mg_2FeH_6 compounds, because of the large differences between Mg and transition metals in melting point and vapor pressure.

Many researches on Mg_2Ni, Mg_2Co, Mg_2Cu and Mg_2FeH_6 compounds revealed that both adding catalysts and nanostructuring are effective ways to improve the hydriding/dehydriding properties of these Mg-based compounds [9–13]. Although catalysts remarkably improve the kinetic properties, they have little effect on the thermodynamic properties. Comparatively, nanostructure benefits to the increased kinetics and the co-existence of chemi-sorption and physi-sorption. Recently, it has been also suggested that when the particle size is reduced to nanoscale, the thermal dynamic properties of hydrogen sorption can be modified by the large surface energy [14–16]. Therefore, nanostructured Mg-based alloys and compounds arises more attention recently [17–21]. For the synthesis of the Mg-based compounds, some technologies have been developed such as ball-milling [17], hydrogen combustion [18], high pressure synthesis [19], thermal evaporation [20] and sputtering [21], but there remain many serious problems such as low generation rate, high impurity and expensive equipments. Moreover it is difficult to get nanostructured Mg-based alloys in large scale. In this regards, it is valuable to develop a new synthesis method for the nanostructured compounds, such as Mg_2Ni, Mg_2Co, Mg_2Cu and Mg_2FeH_6.

Up to now, nanoparticles are usually fabricated by using various chemical and physical methods such as colloidal precipitation, chemical vapor deposition, chloride reduction, roasting of deposited alkali, mechanical attrition, gas-phase condensation [22–26]. The first five methods have the advantages of low production cost, but they have serious problems of low purity and low activity. The most conventional method to product metallic nanoparticles with high purity and good crystallinity is the gas-phase evaporation technique in vacuum or inert-gas of a reduced pressure. Nevertheless, the evaporation rate is quite low in both cases. Thermal plasma is a promising method to solve this problem due to the fact that the evaporation of metal takes place in an atmosphere of active gas [27–30]. The plasmas method is a physicochemical process and offers many unique advantages such as high temperature to enhance the reaction kinetics, high chemical reactivity to form hydride, oxide, and nitride according to different atmosphere, and rapid quenching rate (10^6 K^{-1}) to produce non-equilibrium materials. Moreover, a drastic enhancement of the nanoparticle generation yield has been observed when hydrogen is added to the plasma atmosphere to cause a hydrogen plasma metal reaction (HPMR) [31–35]. In this paper, we will report the fabrication of pure nanoparticles of Mg, Ni, Co, Cu, Fe and other elements by HPMR, the synthesis of nanostructured Mg_2Ni, Mg_2Co, Mg_2Cu and Mg_2FeH_6 compounds by using elemental nanoparticles through a gas–solid reaction, and the hydrogen storage properties of these nanostructured compounds.

2. Experimental

The experimental process is described by a schematic diagram as shown in Fig. 1. To produce nanoparticles, a metal ingot was placed on a water-cooled copper anode plate or a conical graphite anode crucible. A schematic illustration of the HPMR equipment was described previously [36]. The chamber was evacuated to about 10^{-3} Pa, and then a gaseous mixture of Ar and H_2 was fed into the chamber at about 0.1 MPa. When the arc plasma was generated in a current from 100 to 300 A, the metal ingot was melted and nanoparticles were fabricated. The nanoparticles were taken out from the chamber after an enough passivation. The particle size can

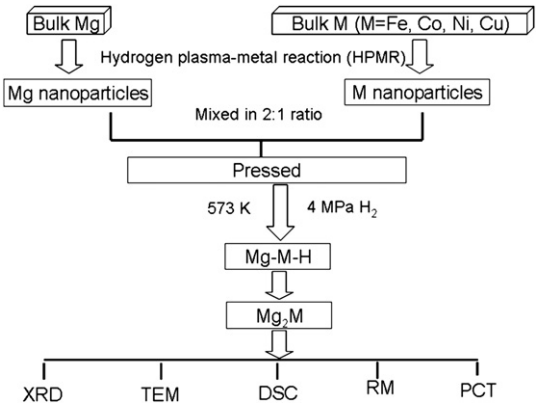

Fig. 1. Schematic diagram of the experimental process.

be tuned by the arc current and hydrogen partial pressure. The structures of these nanoparticles were characterized by X-ray diffraction (XRD) using monochromatic Cu Kα radiation. The size distribution and morphology of these samples were observed by transmission electron microscopy (TEM). The specific surface area was analyzed by BET (Brunauer–Emmett–Teller) method.

To obtain Mg-based compound samples, a mixture of pure Mg and other element metal (M = Ni, Co, Fe, Cu, Al and so on) particles with desirable molar ratio was immersed in acetone and then mixed by an ultrasonic homogenizer for 30 min. After having been dried in the air naturally, the mixed sample was put into a reactor and the system was evacuated to 10^{-3} Pa. Then the sample was heated up to 573 K and hydrogen with a pressure of about 4 MPa was provided to make the mixture of Mg and other metals react with hydrogen for 120 min (one kind of gas–solid reaction). The sample was taken out of the reactor after the system was evacuated to 10^{-3} Pa and cooled to room temperature.

A conventional pressure–volume–temperature technique (Sieverts method), which measures the hydrogen content versus time by recording the gas pressure change in a constant volume, was used to obtain the pressure–composition isotherm curves of the sample at different temperatures. Isotherm measurements of the variation of pressure with time were conducted to obtain the hydrogen sorption kinetics curves. The hydrogen absorption and desorption measurements were thought to reach an equilibrium when the change of hydrogen pressure was less than 10 Pa s^{-1}.

The thermodynamic property of nanostructured Mg_2Ni sample was also studied by DSC measurements using an NETZSCH DSC 204 HP apparatus. Mg and Ni nanoparticle mixture samples of about 10 mg were put into the chamber of the DSC apparatus. After evacuation, hydrogen of 4 MPa was provided to the DSC chamber, and the temperature was increased from room temperature to 823 K at a heating rate of 10 K min^{-1}. The measurement was conducted for 10 cycles after the heating and cooling processes were repeated two cycles. The samples were also annealed for heating and cooling cycles between 453 and 823 K at 5 and 20 K min^{-1} in hydrogen pressure of 4 MPa, respectively.

3. Results and discussions

3.1. Fabrication of nanoparticles by hydrogen plasma metal reaction

Fig. 2 shows the TEM images of the selected Mg, Ni, Cu, Co, Fe and Al nanoparticles produced by HPMR. Table 1 summarizes the

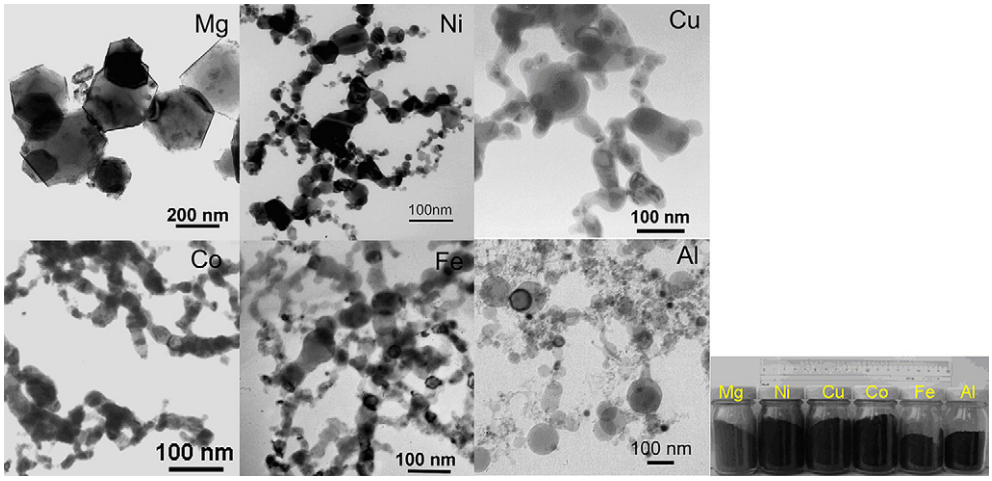

Fig. 2. TEM images of various metal nanoparticles and photo of nanoparticle samples.

yield rate, phase and particle size of these nanoparticles. All these particles are nearly spherical in shape. The mean particle size of Mg is 540 nm, whereas the other elements are in the range of 20–50 nm. Mg particles have a larger size than the other elements because of the larger yield rate of Mg particles during HPMR. The yield rate is essentially determined by the evaporation speed and the saturation vapor pressure of pure element metals. As to the main group metals and transition metals, the evaporation speed is approximately proportional to the reaction parameter Rp, which can be calculated with the following equation [37]:

$$Rp = -\frac{\Delta H_r}{L_s} \cdot \frac{N_{H_2}(T)}{N_{H_2}(273)} \quad (1)$$

where ΔH_r is the reaction enthalpy between hydrogen and the metal, L_s is the vaporization heat of the metal at temperature T, $N_H(T)$ and $N_H(273)$ are the densities of molecular hydrogen in metal at temperature T and 273 K, respectively. With this formula, the reaction parameter of Mg is evaluated to be about 18 times larger than those of other metals. This is why Mg has much larger yield rate and particle size.

The plasma in HPMR is composed of a lot of hydrogen ions and neutral atoms, which can dissolve into the melted metal in a much larger quantity than hydrogen in the normal gas status. After entering the melted metal, they will release energy and electric charges, and combine into hydrogen molecules. Finally, they get saturation and are released from the melted metal, which results in the metal evaporation remarkably. Fig. 3 displays the schematic illustration of the nanoparticle formation during HPMR, which contains the following five steps: (1) the dissociation of diatomic molecular hydrogen in plasma zone; (2) the dissolve of hydrogen ions and neutral atoms into the molten metals; (3) the oversaturation of hydrogen atoms, the combination into hydrogen molecules in the molten metals, and the formation of hydrogen bubbles; (4) the escape of hydrogen bubbles from the molten metals together with metal vapor in them; (5) the metallic vapor condensation and nanoparticle formation.

When the hydrogen percentage is lower than 50%, the hydrogen bubble evaporation rate increases with the increasing hydrogen partial pressure. At higher hydrogen content, the evaporation rate almost reaches saturation. To get the largest nanoparticle generation yield and stable plasma state, the optimal hydrogen percentage should be 20–50%. Since the preparation process can be continuously carried out, this technique is possible to fabricate metallic nanoparticles in large scale as shown in the photo of Fig. 2. The composition analysis proves that the oxygen content is lower than 1% in all the samples including the active Mg particles, which is attributed to the strong reducibility of the hydrogen plasma and the enough passivation treatment. From Table 1, it can be seen that pure metallic nanoparticles are obtained in the non-hydride formation elements such as Fe, Co, Ni, Cu and Al, but metal hydride nanoparticles are obtained in the hydride-formation elements such as Ti, Zr, Ce, Sm except for Mg. Hydrogen plasma is a strong hydriding atmosphere and the particles prepared by this process are small in size, so the hydrogenation should be easy to

Table 1
Characteristics of various metal nanoparticles.

Element	Preparation atmosphere	Yield rate (g h^{-1})	Phase	Mean particle size (nm)
Mg	20% H_2 + 80% Ar	86.5	Mg (hcp)	540
Ti	50% H_2 + 50% Ar	8.3	$TiH_{1.9}$ (fcc)	22
Ce	20% H_2 + 80% Ar	12.5	CeH_2 (fcc)	55
Sm	20% H_2 + 80% Ar	32.6	Sm_3H_7 (fcc)	43
Fe	50% H_2 + 50% Ar	5.5	Fe (bcc)	39
Co	50% H_2 + 50% Ar	5.1	Co (fcc)	37
Ni	50% H_2 + 50% Ar	3.0	Ni (fcc)	33
Cu	50% H_2 + 50% Ar	2.6	Cu (fcc)	31
Al	50% H_2 + 50% Ar	11.2	Al (fcc)	58

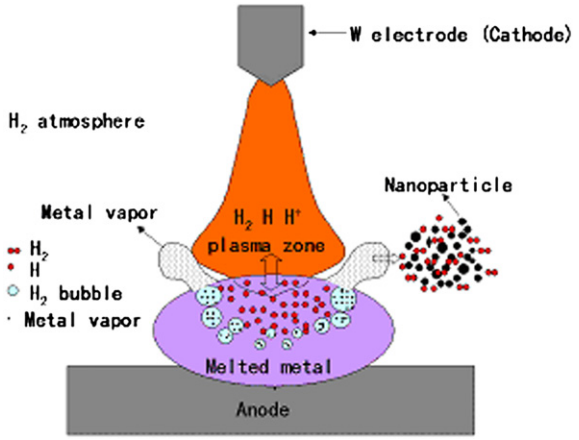

Fig. 3. Schematic illustration of the nanoparticle formation and hydrogenation.

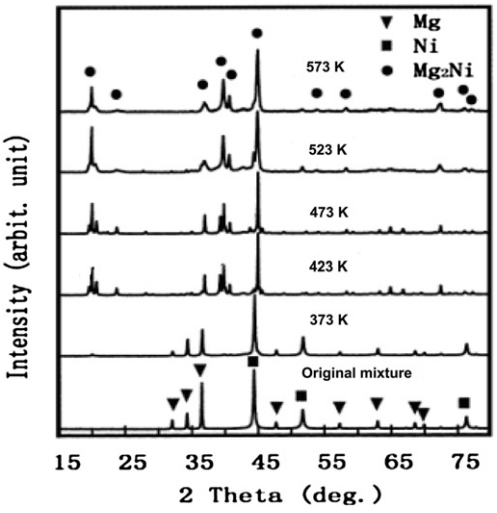

Fig. 4. XRD patterns of 2 Mg + Ni particles heated at different temperatures.

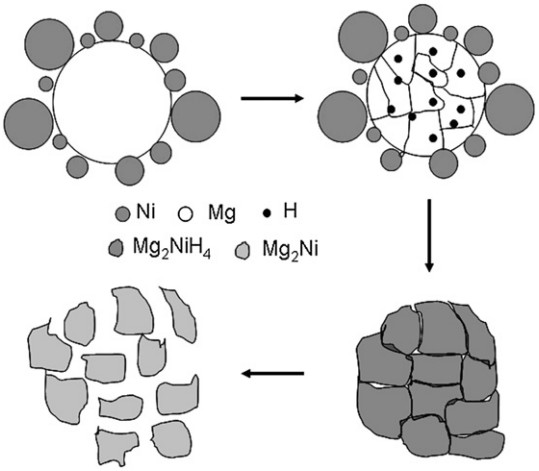

Fig. 6. Schematic illustration of the gas–solid reaction of the Mg-based compound nanoparticles.

take place for the hydride-formation elements. The hydrogen–magnesium reaction is a nucleation and growth process where the nucleation rate of magnesium hydride is dependent mainly on hydrogen pressure. The hydrogenation of Mg usually takes place at high hydrogen pressure of several tens of bars, much higher than other hydride-formation elements. At the plasma region, thermodynamically the magnesium vapor is unable to react with the reactive H atom under such high temperature. Outside the plasma region, although the fresh surfaces, large surface areas and higher activity of the ultrafine Mg particles are helpful for the hydrogen uptake, the low pressure of 0.05 MPa and high cooling rate in HPMR result in rather low nucleation rate of magnesium hydride and the formation of Mg instead of magnesium hydride.

3.2. Fabrication of nanostructured Mg_2M (M = Ni, Co, Cu) and Mg_2FeH_6 by gas–solid reaction

By using the particles prepared by HPMR as the initial materials, we prepared the nanostructured Mg_2M and Mg_2FeH_6 compounds. Fig. 4 shows the XRD patterns of a mixture of magnesium and nickel particles in 2:1 molar ratio after being annealed in 4 MPa H_2 at different temperatures and then evacuated at room temperature. It is surprising to find that Mg_2Ni start to form even at 423 K, and pure Mg_2Ni is obtained at 523 K, much lower than the temperature in the hydride combustion synthesis [38,39]. From Fig. 5B, it can be seen that the particle size of Mg_2Ni is about 50 nm, which is even smaller than the original Mg particles (see Fig. 5A). This can be explained by the hydrogen-induced disintegration as shown in Fig. 6. The Mg particles absorb hydrogen quickly with Ni as catalyst, and they disintegrate into smaller particles during the hydrogenation/dehydrogenation process. Moreover, the formation of Mg_2Ni during the dehydrogenation at a low temperature maintains its original nanostructure. Since Ni is not able to absorb hydrogen and disintegrate like Mg during the fabrication of the nanostructured Mg_2Ni, it is more important for Ni to possess a particle size in nanoscale. L.Q. Li et al. successfully synthesized Mg_2Ni by hydrogen combustion [38,39], which was more convenient than normal mechanical alloying, especially for the large-scale preparation. However, since the combustion temperature is higher than 750 K, the grain size is as large as several tens of micrometers. The subsequent ball-milling is usually required to get fine microstructure and good hydrogen absorption properties. In contrast, in this study, the nanostructured Mg_2Ni can be directly produced without ball-milling because the interdiffusion and combination of Mg and Ni can take place at a quite low temperature.

Fig. 7 shows the XRD patterns of the mixed Mg and Ni particles after being heated at 573 K in 4 MPa H_2 for different times. From this figure, it can be seen that Mg particles firstly react with

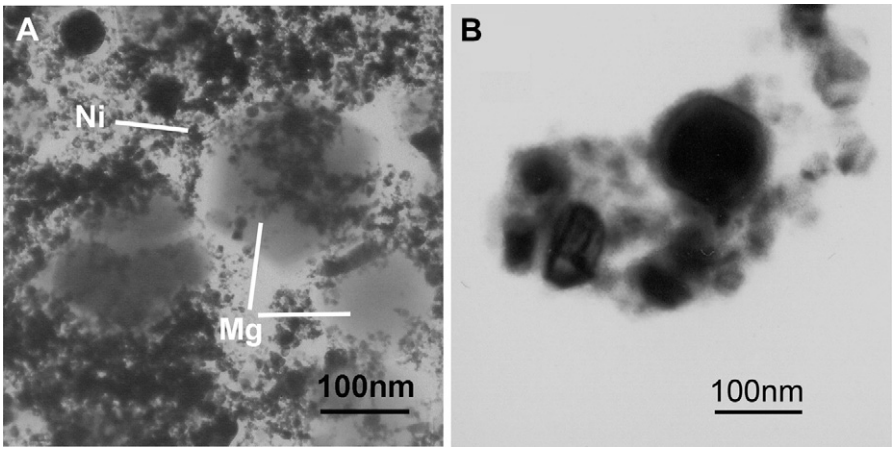

Fig. 5. TEM micrographs of the mixture of Mg and Ni particles (A) and the Mg_2Ni nanoparticles prepared at 573 K in hydrogen atmosphere (B).

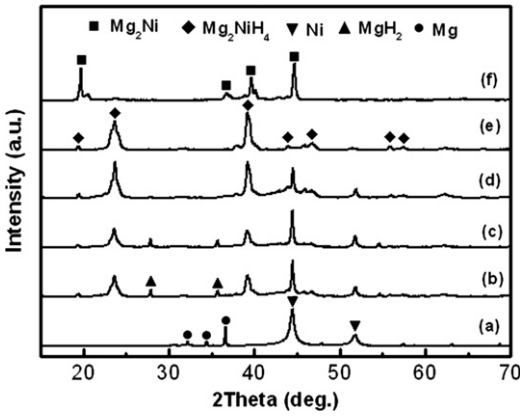

Fig. 7. XRD patterns of 2 Mg + Ni particles heated at 573 K at different times in 4 MPa H_2: (a) 0 min, (b) 15 min, (c) 30 min, (d) 1 h and (e) 2 h; and after dehydrogenation (f).

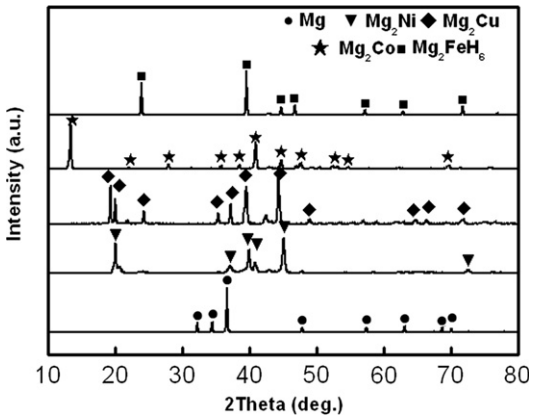

Fig. 8. XRD patterns of Mg_2Ni, Mg_2Cu, $MgCo_2$ and Mg_2FeH_6 samples prepared by gas–solid reaction.

hydrogen to form MgH_2 with Ni as a catalyst, which has been reported previously [40]. Then MgH_2 reacts with Ni to become the compound hydride Mg_2NiH_4. Finally, the hydride desorbs hydrogen during evacuation to produce Mg_2Ni compound. It is worth noting that Mg particles can absorb hydrogen rapidly when mixed with Ni nanoparticles, implying the important catalytic effect of Ni nanoparticles on the hydrogenation of Mg. The processes can be expressed by the following equations:

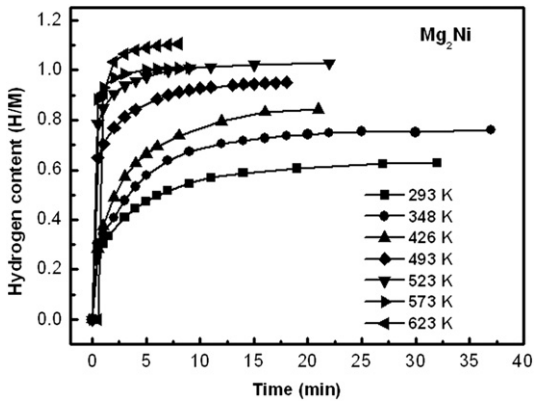

Fig. 9. Hydrogen absorption and desorption curves of Mg_2Ni nanoparticles at different temperatures.

$$\text{Mg hydride formation}: Mg + H_2 \rightarrow MgH_2 \quad (2)$$

$$\text{Mg} - \text{based Compound hydride formation}: 2MgH_2 + Ni \rightarrow Mg_2NiH_4 \quad (3)$$

$$Mg_2Ni \text{ formation during hydrogen desorption}: Mg_2NiH_4 \rightarrow Mg_2Ni + 2H_2 \quad (4)$$

The similar experiment for Mg and Ni particles in micrometer order was conducted at 573 K in 4 MPa H_2 even for 24 h, but Mg_2Ni was not obtained. The increase of reaction temperature is able to promote the diffusion of metallic atom, however, this will induce particle enlargement. Therefore, the fine particle size is crucial for this gas–solid reaction. From our previous study [41], it was known that hydrogen-induced amorphization (HIM) occurred during the low temperature gas–solid reaction in many rare earth-based intermetallic compounds when the hydrogen content reached 1.3 H M^{-1}. In the case of Mg–Ni, however, HIM does not occur, indicating that the interdiffusion and crystallization in Mg–Ni system are easier than those in rare earth elements.

Via the same approach, we synthesized other Mg-based compounds. Fig. 8 shows the XRD patterns of Mg, Mg_2Ni, Mg_2Co, Mg_2Cu and Mg_2FeH_6. It is quite difficult to prepare the pure phase samples of these compounds by other techniques. From Fig. 8, it is apparently seen that all these compounds are successfully

Table 2
Formation conditions and characteristics of Mg_2M compounds.

Compounds	Reaction process	Temp. (K)	Crystalline structure and lattice constants (Å)	Mean particle sizes (nm)
Mg_2Ni	$Mg + H_2 \rightarrow MgH_2$ $MgH_2 + Ni \rightarrow Mg_2NiH_4$ $Mg_2NiH_4 \rightarrow Mg_2Ni$ $Mg_2Ni + H_2 \leftrightarrow Mg_2NiH_4$	573	Hexagonal Primitive $a = 5.205$ $c = 13.23$	50
Mg_2Cu	$MgH_2 + Cu \rightarrow Mg_2Cu + H_2$ $Mg_2Cu + H_2 \leftrightarrow MgH_2 + MgCu_2$	673	Orthorhombic Face-centered $a = 9.07$, $b = 18.24$, $c = 5.283$	300
Mg_2Co	$MgH_2 + Co + H_2 \rightarrow Mg_2CoH_5$ $Mg_2CoH_5 \rightarrow Mg_3CoH_5$ $Mg_3CoH_5 \rightarrow Mg_2Co$ $Mg_2Co + H_2 \leftrightarrow Mg_3CoH_5 \leftrightarrow Mg_2CoH_5$	623	Cubic Face-centered $a = 11.43$	200
Mg_2FeH_6	$Mg + H_2 \rightarrow MgH_2$ $MgH_2 + Fe + H_2 \leftrightarrow Mg_2FeH_6$	673	Cubic Face-centered $a = 6.43$	200

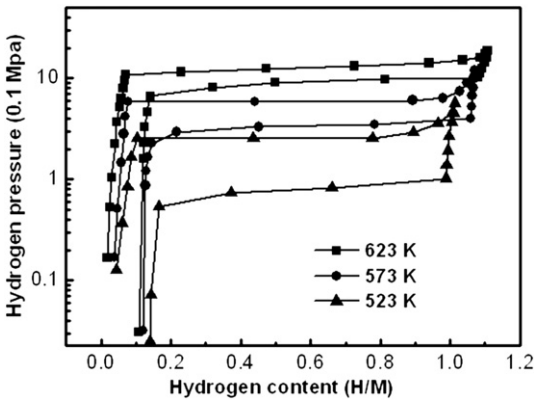

Fig. 10. Pressure–composition isotherm curves of Mg_2Ni nanoparticles at different temperature.

produced in this study, indicating that the gas–solid reaction in nanoscale is an effective way to synthesize Mg-based compounds. Moreover, different from mechanical alloying, single phase and nanostructured Mg-based compounds are directly obtained in this work. This technology can be further used to prepare other compounds as well as composite materials, much more convenient than other methods. The formation condition and characteristics of Mg_2M (M = Ni, Cu, Co) and Mg_2FeH_6 compounds are summarized in Table 2. It can be seen that the formation mechanisms of these Mg-based compounds are similar to Mg_2Ni. Mg particles first form hydride and then react with transition metals to form Mg_2M hydride. After dehydriding, the intermetallic compounds Mg_2M are produced. Since the stable Mg–Fe compounds do not exist on the basis of Mg–Fe binary equilibrium phase diagram, only the nanostructured Mg_2FeH_6 can be prepared upon hydrogenation. The mean particle size of these compounds changes from 50 to 300 nm, which is probably due to the differences in the reaction temperature and the catalytic effects of transition metals on hydrogen decomposition.

3.3. Hydrogen storage properties of Mg_2M

The hydrogen absorption rates of the nanostructured Mg_2Ni at different temperatures are given in Fig. 9. The vertical axis represents the hydrogen content in the form of H/M. It is found that the nanostructured Mg_2Ni sample can even absorb 0.6 H M^{-1} hydrogen at room temperature. At 493 K, the sample absorbs hydrogen quickly and approaches a saturation value of 0.95 H M^{-1} in several minutes. Mg_2Ni particles in micrometer absorb hydrogen very slowly below 523 K even under catalyst assistant [42–44]. For the nanostructured Mg_2Ni, the hydrogen absorption rate is quite fast, and the absorption temperature is lower than that of the Mg_2Ni in micrometer reported before. The pressure–composition isotherm curves in Fig. 10 exhibit clear equilibrium plateaus in both absorption and desorption processes, and the hydrogen storage capacity is close to the theoretical value. The equilibrium plateau pressures are slightly higher than those of the conventional magnesium nickel compound. The results of the absorption temperature, the absorption rate and the equilibrium plateau pressure indicate that the nanostructure improves the hydrogen storage properties of Mg_2Ni. Similar results are also observed in other Mg-based compounds.

In order to understand the kinetic and thermodynamic properties and the cyclic property, we studied the nanostructured Mg_2Ni by the high pressure DSC in hydrogen atmosphere, as shown in Fig. 11. There are two endothermic peaks in the heating process and two exothermic peaks in the cooling process, respectively. The sharp peaks at 687 and 721 K correspond to hydrogen absorption and desorption, respectively. The small peaks at 500 and 510 K correspond to a phase transformation of Mg_2NiH_4 between a high temperature cubic structure and a low temperature monoclinic phase [45,46]. From the peak areas of hydrogen absorption and desorption, the enthalpy changes of these two peaks are calculated to be 63.1 and 64.2 kJ mol^{-1} H_2, respectively. By using different heating rates of 5, 10, 20 K min^{-1} in the DSC measurements, we obtained the activation energy of the hydrogenation, $E_a = 66.0$ kJ mol^{-1} H_2, which is much smaller than that reported on the micro-size Mg_2Ni of 88.32 kJ mol^{-1} H_2 [47]. From Fig. 11(b), it can be seen that all the peaks of hydriding and dehydriding repeat

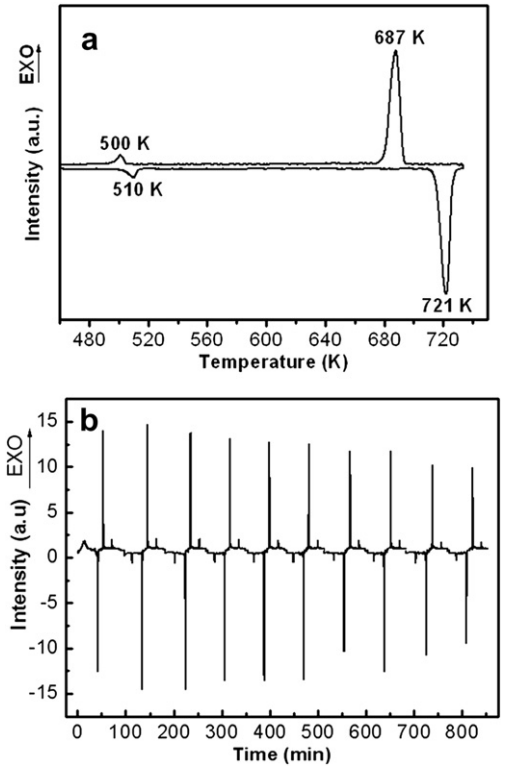

Fig. 11. The high pressure DSC measurement of 2 Mg + Ni particles in 4 MPa hydrogen atmosphere at a heating rate of 10 K min^{-1} in the first cycle (a) and the comparison of DSC curves between the first and tenth cycles (b).

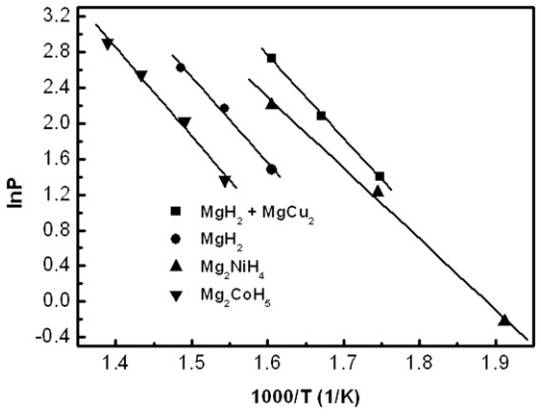

Fig. 12. Plot of plateau pressure vs. temperature for Mg_2M compounds and MgH_2.

Table 3
Hydride formation enthalpy and entropy of Mg-based compounds.

Hydrides	Van't Hoff equation	Enthalpy (ΔH) kJ mol^{-1} H_2	Entropy (ΔS) J K^{-1} mol^{-1} H_2
MgH_2	ln (P/0.1 Mpa) = −9604/T + 16.93	−79.80	−140.8
Mg_2NiH_4	ln (P/0.1 Mpa) = −7977/T + 15.07	−66.32	−125.3
Mg_2CoH_5	ln (P/0.1 Mpa) = −9895/T + 16.70	−82.27	−138.8
$MgH_2 + MgCu_2$	ln (P/0.1 Mpa) = −9275/T + 17.61	−77.11	−146.4

well and shift little during ten cycles, indicating that the sorption kinetics of the nanostructured Mg_2Ni is relatively stable and it has excellent cycling property. However, the peak intensity declines slightly with circulation, and the corresponding peak area decreases to 58.1 kJ mol^{-1} H_2 in the tenth cycle. It is suggested that one possible reason for the decreased peak area is the growth of particle size of the nanostructured Mg_2Ni during the cycling, which slightly decreases the sorption kinetics. The hydriding and dehydriding of large Mg_2Ni particles take place mainly in the surface layer during the rapid heating process, and the particle core does not contribute to the reaction, leading to the slight decrease of peak area in the DSC curve. Therefore, in order to keep the excellent cycling property of the nanostructured Mg-based compounds, it is crucial to inhibit the particle growth.

On the basis of the pressure–composition isotherm curves of these nanostructured Mg-based compounds, the equilibrium plateau pressures at different temperatures are summarized in Fig. 12. According to van't Hoff equation shown below, the hydride formation enthalpy ΔH and entropy ΔS are calculated and given in Table 3.

$$\ln P_{H_2} = 2\Delta H/nRT - 2\Delta S/nR \quad (5)$$

where, n is the reaction order, R the gas constant, T temperature. The enthalpies and entropies of these nanostructured Mg-based compounds are slightly lower than those reported elsewhere [48–51]. This means that the hydrogen bonding state in the nanostructured Mg-based hydrides is weakened and easy to be released. It can also be concluded that the thermodynamics of hydriding/dehydriding is not greatly improved with the decrease of particle size as the kinetics. For getting greater thermodynamic improvement, the particle size should be decreased further, possibly smaller than 20 nm. A detailed study about this is now in progress.

4. Conclusion

HPMR is effective to prepare nanoparticles of Mg and other transition metals in large scale because of plasma promotion. The nanoparticle formation process can be divided into five steps: the formation of active hydrogen ion or atom, the hydrogen oversaturation dissolving, the hydrogen bubble formation, the evaporation of metal vapor together with hydrogen bubble and the condensation of metal vapor. Metallic nanoparticles are fabricated by HPMR method when the starting metal is a non hydride formation element, whereas metal hydride nanoparticles are produced when the starting metal is a hydride formation element except for Mg.

The pure and nanostructured Mg_2Ni, Mg_2Co, Mg_2Cu and Mg_2FeH_6 have been successfully prepared by gas–solid reaction of hydrogen and mixture of Mg and corresponding transition metal nanoparticles. The reaction temperature is much lower than the hydrogen combustion approach, therefore, the nanostructure can be kept through the reaction. The hydrogen absorption and desorption rates are promoted and the sorption temperatures are decreased. The kinetic properties are improved greatly because of the short diffusion distance and large specific surface area. The thermodynamic properties of the nanostructured Mg_2M are improved only slightly.

Acknowledgments

The authors acknowledge NSFC (No. 20971009 and 51071003), MOST of China (No. 2010CB631301 and 2011AA03A408), MOE of China (No. 707002), the Aeronautical Science Foundation of China (No. 2009ZF51062 and 2011ZF51065), Delta Electronics INC and the Scientific Research Foundation for the Returned Overseas Chinese Scholars, State Education Ministry.

References

[1] S.I. Orimo, Y. Nakamori, J.R. Eliseo, A. Zuttel, C.M. Jensen, Chem. Rev. 107 (2007) 4111–4132.
[2] H.Y. Leng, T. Ichikawa, S. Hino, N. Hanada, S. Isobe, H. Fujii, J. Power Sources 156 (2006) 166–170.
[3] P. Ngene, R. Berg, M. Verkuijlen, K. de Jong, P. de Jongh, Energy Environ. Sci. 4 (2011) 4108–4115.
[4] J. Cermak, L. Kral, J. Power Sources 197 (2012) 116–120.
[5] N.S. Norberg, T.S. Arthur, S.J. Fredrick, A.L. Prieto, J. Am. Chem. Soc. 133 (2011) 10679–10681.
[6] M.G. Veron, F.C. Gennari, G.O. Meyer, J. Power Sources 195 (2010) 546–552.
[7] J. Muldoon, C.B. Bucur, A.G. Oliver, T. Sugimoto, M. Matsui, H.S. Kim, G.D. Allred, J. Zajicek, Y. Kotani, Energy Environ. Sci. 5 (2012) 5941–5950.
[8] T. Ozaki, M. Kanemoto, T. Kakeya, Y. Kitano, M. Kuzuhara, M. Watada, S. Tanase, T. Sakai, J. Alloys Compd. 446 (2007) 620–624.
[9] R.A. Varin, T. Czujko, Z.S. Wronski, Nanomaterials for Solid State Hydrogen Storage, Springer Science Business Media, New York, 2009.
[10] M. Conte, P.P. Prosini, S. Passerini, Mat. Sci. Eng. B 108 (2004) 2–8.
[11] W.Y. Li, C.S. Li, H. Ma, J. Chen, J. Am. Chem. Soc. 129 (2007) 6710–6711.
[12] M. Latroche, J. Phys. Chem. Solids 65 (2004) 517–522.
[13] M. Bououdina, D. Grant, G. Walker, Int. J. Hydrogen Energy 31 (2006) 177–182.
[14] R.W.P. Wagemans, J.H. van Lenthe, P.E. de Jongh, A.J. van Dillen, K.P. de Jong, J. Am. Chem. Soc. 127 (2005) 16675–16680.
[15] V. Berube, G. Radtke, M. Dresselhaus, G. Chen, Int. J. Energy Res. 31 (2007) 637–663.
[16] K.C. Kim, B. Dai, J.K. Johnson, D.S. Sholl, Nanotechnology 20 (2009) 204001.
[17] J. Yang, M. Ciureanu, R. Roberge, J. Alloys Compd. 287 (1999) 251–255.
[18] L.Q. Li, T. Akiyama, J. Yagi, J. Alloys Compd. 308 (2000) 98–103.
[19] D. Moser, D.J. Bull, T. Sato, D. Noreus, D. Kyoi, T. Sakai, N. Kitamura, H. Yusa, T. Taniguchi, W.P. Kalisvaarte, P. Notten, J. Mater. Chem. 19 (2009) 8150–8161.
[20] H. Wang, L.Z. Ouyang, M.Q. Zeng, M. Zhu, J. Alloys Compd. 375 (2004) 313–317.
[21] J.L. Qu, Y.T. Wang, L. Xie, J. Zheng, Y. Liu, X.G. Li, Int. J. Hydrogen Energy 34 (2009) 1910–1915.
[22] S. Mandan, D. Rautaray, M. Sastry, J. Mater. Chem. 13 (2009) 3002–3005.
[23] K. Akamatsu, S. Deki, Nanostruct. Mater. 8 (1997) 1121–1129.
[24] Y.Y. Yu, S.S. Chang, C.L. Lee, C.R.C. Wang, J. Phys. Chem. B 101 (1997) 6661–6664.
[25] N.S. Sobal, M. Hilgendorff, H. Mohwald, M. Giersig, M. Spasova, T. Radetic, M. Farle, Nano Lett. 2 (2002) 621–624.
[26] G. Krishnan, G. Palasantzas, B.J. Kooi, Appl. Phys. Lett. 97 (2010) 261912.
[27] K. Nakahigashi, H. Ishibashi, S. Minamigawa, M. Kogachi, Jpn. J. Appl. Phys. 31 (1992) 2293–2298.
[28] V.I. Konov, A.A. Smolin, V.G. Ralchenko, S.M. Pimenov, E.D. Obraztsov, E.N. Loubnin, S.M. Metev, G. Sepold, Diam. Relat. Mater. 4 (1995) 1073–1078.
[29] X.L. Dong, Z.D. Zhang, X.G. Zhao, Y.C. Chuang, S.R. Jin, W.M. Sun, J. Mater. Res. 14 (1999) 398–406.
[30] T. Watanabe, H. Itoh, Y. Ishii, Thin Solid Films 390 (2001) 44–50.
[31] T. Liu, T.W. Zhang, X.Z. Zhang, X.G. Li, Int. J. Hydrogen Energy 36 (2011) 3515–3520.
[32] T. Liu, T.W. Zhang, C.G. Qin, M. Zhu, X.G. Li, J. Power Sources 196 (2011) 9599–9604.
[33] X.G. Li, A. Chiba, S. Takahashi, M. Sato, J. Appl. Phys. 83 (1998) 3871–8753.
[34] X.G. Li, A. Chiba, M. Sato, S. Takahashi, Acta Mater. 51 (2003) 5593–5600.
[35] T. Liu, C.G. Qin, T.W. Zhang, Y.R. Cao, M. Zhu, X.G. Li, J. Mater. Chem. 22 (2012) 19831.
[36] T. Liu, T.W. Zhang, M. Zhu, C.G. Qin, J. Nanopart. Res. 14 (2012) 738–745.
[37] S. Ohno, M. Uda, Trans. Jpn. Inst. Met. 48 (1984) 640–646.

[38] L.Q. Li, I. Saita, T. Akiyama, J. Alloys Compd. 384 (2004) 157–164.
[39] L.Q. Li, I. Saita, T. Akiyama, Intermetallics 13 (2005) 662–668.
[40] G. Liang, J. Huot, S. Boily, A. Van Neste, R. Schulz, J. Alloys Compd. 292 (1999) 247–252.
[41] X.G. Li, A. Chiba, K. Aoki, T. Masumoto, J. Alloys Compd. 255 (1997) 253–261.
[42] S.Y. Zheng, F.J. Zhang, L.X. Sun, B. He, S.Q. Wei, G.R. Chen, D.L. Sun, J. Phys. Chem. C 111 (2007) 14021–14025.
[43] S.H. Hong, S.N. Kwon, J.S. Bae, M.Y. Song, Int. J. Hydrogen Energy 34 (2009) 1944–1950.
[44] C.Y. Chen, C.K. Wang, P.Y. Lee, C.K. Lin, Mater. Trans. 48 (2007) 3170–3175.
[45] D. Noreus, L.G. Olsson, J. Chem. Phys. 78 (1983) 2419–2427.
[46] M. Gupta, E. Belin, L. Schlapbach, J. Less-Common Met. 103 (1984) 389–399.
[47] J.S. Han, J.Y. Lee, J. Less-common Met. 131 (1987) 109–116.
[48] D.L. Sun, H. Enoki, F. Gingl, E. Akiba, J. Alloys Compd. 285 (1999) 279–283.
[49] J.J. Reilly, R.H. Wiswall, Inorg. Chem. 7 (1968) 2254–2256.
[50] K. Nomura, E. Akiba, S. Ono, Int. J. Hydrogen Energy 6 (1981) 295–303.
[51] K.J. Gross, P. Spatz, A. Züttel, L. Schlapbach, J. Alloys Compd. 240 (1996) 206–213.